Physical Parametric Studies of Photonic Crystal Cavity Affecting the Performances of Sensor Applications

Nuraini Liyana Binti Mohd Shafri

Faculty of Electrical Engineering, Universiti Teknologi Mara (UiTM), Shah Alam, July 2017.

Abstract – In this work, a small size of PC slab high sensitivity, and high accuracy sensor for measuring the performance of sensor application was realized in variation of sensing material such as cryptophane E, sugar-water solution and phosphate buffered saline (PBS) infiltrated photonic crystal cavity (PhCC) by combining selective absorption characteristic of sensing material to gas, liquid and protein sensor. The parametric studies has been done by increased the refractive index (RI) of the different sensing material, increase the number of defected holes of PhCC and increase the radii of defected holes of the PhCC. The RI of different sensing material that infiltrated in defected holes of PhCC will induce a shift of resonant wavelength and allowing the precision absorption characteristic in different sensor application. In order to demonstrate the parametric studies based on 2D silicon PhCC, we used the finite difference time domain (FDTD) method to observe the performance of PhCC sensors. The simulation results of PhC microcavity for gas sensing show the RI sensitivity of 48.2 nm/RIU, a quality factor of 2551 and transmission of 0.3330. Liquid sensing simulation results shows the RI sensitivity of 46.3 nm/RIU, a quality factor of 1874 and transmission of 0.5690. In protein sensing results show, the RI sensitivity of 114.4 nm/RIU, quality factor of 1659 and transmission of 0.3814. The advantage of high sensitivity and high quality factor of the PhC microcavity which is, it can be used in other sensing material as well, and protein showed highest RI sensitivity value of 114.4 nm/RIU. The design has been realized in silicon photonic crystal structure. The whole design and simulation process is done by using the OptiFDTD software.

1.0 INTRODUCTION

Malaysia has stated in one of the lowest polluted city environments in Asia. Malaysia goals are to achieve one of the industrial countries in the year 2020 and has rapid economic growth have started to implement costs to the industrial pollution and the degradation of a city environment. Recently, the issues of air, water pollution, and contamination become more serious in Malaysia. Most of these waste has come from the industrial sector. From all types of pollutions, air pollution is the biggest issue because the effects of this pollution can affect human health, agricultural crops, forest species and also ecosystems [1]. In order to prevent the harmful of this air pollution, the concentration of these dangerous air polluting gases or known as haze gaseous such as methane need to be monitored. For example, in the medical sector, the Ethanol breathe testing in respiratory gas need to be monitored and controlled. There are several types of gas detectors in the market such as, the gas detector that has been used to measures the changes in the conductance or in the capacitance brought by the presence of certain gas atoms that are absorbed onto the surface or diffuse into the detector material. However, most of this method are limited to the certain specific gases that influence the physical properties of the detector materials. Another type of detectors is optical or usually known as spectroscopic gas sensors. This gas sensor measured the changes of reflection or transmission in the presence of gases. In this method, the characteristic of absorption lining arising such as from rotational and vibrational excitations of molecules in the mid-infrared (MIR) spectral range has been monitored. The principal of spectroscopic is generally applicable to a variety of gases and it is highly selective due to the specific rotational-vibrational states. However, because of the high cost due to the high demand on optical component make this optical sensor become a major drawback to the industry [2].

A spectroscopic gas sensor contains three basic parts which are the interaction source, the interaction volume, and the radiation detector. For example, the using of laser sources and adapted detectors as to build a very sensitive, selective and fast instruments [3]. By employing the tunable laser spectroscopy, the precisely tune of a monochromatic intense laser emission line across gas absorption lines has been detected. The combination of collimated laser beams and Harriot multi-reflection cells, resulting in the interaction lengths of 100 m and above [4]. Therefore, in the example of the sensitivities in the parts per trillion range can be achieved with the quantum cascade laser (QCLs) in the MIR range [3]. The effective interaction lengths of several kilometers have been demonstrated and also yield ppt sensitivity is by using the cavity ring down or cavity leak out setups [5]. However, in most cases, due to the high price of the laser and other system components, thus it is prohibit and limits these technique to niche applications. The low-cost thermal

emitters and thermopile or pyroelectric detectors are the majority of optical gas sensors that are used as a radiation sources in detectors with adapted optical components. Therefore, the Photonic crystals cavity (PhCC) can be used to obtain compact, strong, and low-cost spectroscopic gas sensor and the interaction of volume has been considered to replace as a conventional sensor by PhCC.

2.0 LITERATURE REVIEW

The photonic crystal dimensionality is firstly analysed theoretically in early 1887 by Lord Rayleigh which is state that the multilayer dielectric stack is the simplest example in 1D PhC [6]. 1D PhC also was known as Bragg mirrors, in which its optical structures consists of alternating layers of high and low refractive index materials. Besides that, the concept of photonic bandgaps also existing in two and three-dimensional structures which are introduced by Yablonovitch et al [7] and John et al [8]. The 2D PhC consists of a dielectric crystal pattern that is periodic throughout a two-dimensional plane with the photon propagation is confined only to that plane. There are two implementations exist in 2D PhC that are PhC fibers and slab-PhCs. The PhC fibers are approximate an infinite thick projection of 2D PhC pattern and their bandgap properties of 2D PhC structure are used to guide light along the length of the fiber. The used of PhC fibers is for physical and biochemical sensing [9] [10]. Another 2D PhC which is slab-PhCs is more closely approximate the zero-thickness case. The thickness of the dielectric materials in the third dimension for these devices is naturally on the order of the crystal lattice spacing, and light confinement in that direction results from the total internal reflection (TIR).

The 2D slab photonic crystals are essentially a 2D periodic array of structural features that was made from an otherwise uniform thin layer of dielectric material. The propagation of light through a slab-PhC is controlled laterally in the plane of the slab by the photonic band properties of the PhC. Light propagation is controlled in the direction perpendicular to the slab by TIR. Therefore, the dielectric layer from which the PhC is made must have refractive index (R1) is higher than the surrounding material. Slab-PhCs have been implemented in sensing experiments which the dielectric layer material either polymer or semiconductor (R1> -1.45) immersed in either gaseous or aqueous environment (R1 < -1.45). There are two common structural arrangements that are often used in producing slab-PhC that are a lattice of high-R1 pillars in a low-R1 cover material and a lattice of low-R1 holes in a high-R1 slab. Fig.1 below is the schematic example of this two geometrics.

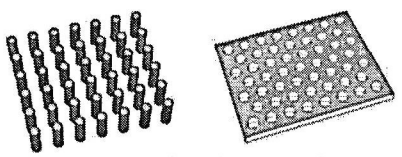

Fig.1: 2D slab PhC geometry schematics representing a square lattice of high-R1 pillars (left) and a triangular lattice of low-R1 holes in a high-R1 dielectric layer (right).

As a typical structure type, the point defect that has been introduce in the orderly arranged lattices shows how the PC cavity formed. A high quality factor (Q) is the strong interaction strength between the optical field and the defected region of the material to show the strong spatial of light confinement and long photon lifetime [11]. Therefore, for sensing application this enhancement gives rise to an optical mode of PCC with a resonant wavelength that is highly sensitive to the local variations in its surrounding medium, and produce PCC as a building block for high-sensitivity optical sensor [12]. There are several important resonant parameters and sensing principle that will affect the performance of the PCC. For example, the shoulder-coupled cavity that published in Ref. [13]. To begin, the property of PC waveguide (PCW) need to be analyse, which is formed by removing the central row of air holes from the perfect PC along x direction. These parameters is shown in the Fig.3 where a is the lattice constant, r is the radius of air hole, d is the waveguide width, and h is the slab thickness. Its basic principle is that light which is located in PBG can only be guided in the line waveguide as it is confined horizontally by PBG of PC and vertically by total internal reflection due to the differences of RI between different layers.

In this research, a micro RI sensor is designed in a 2D PhCC with a triangular lattice. The radius of air holes is careful to be designed in order to realize high sensitivity and appropriate measurement range. The microcavity can be formed by varying the radius of center air holes. In the other hand, the higher transmission efficiency can be realized by optimizing the parameters of the waveguides. The sensor also needs to have high transmission efficiency and Q factor, which is could make the detection easy and feasible. There are three important performances in sensing application:

i) RI Sensitivity, S_n

In order to analyze the RI sensitivity of the PhC microcavity structure, the resonant wavelength shift ($\Delta\lambda$) and the variation of refractive index (Δn) need to be observed. RI sensitivity can be expressed as follows:

$$S = \Delta\lambda/\Delta n \qquad (2.1)$$

The slope of each curve for each refractive index represents the sensitivity of the specified PhC microcavity. In theoretically, the largest slope and maximum sensitivity will occur for larger radius of defected holes [14].

ii) Q factor, Q

Quality factor can be calculated by dividing the resonant wavelength (λ) with the full width at half-maximum (FWHM) of the drop waveguide output ($\Delta\lambda$) or can be calculated by using Equation (2.2) [15]. Q factor can be expressed as:

$$Q = \frac{f_o}{f_2 - f_1} \qquad (2.2)$$

The resonant wavelength and the bandwidth can be measured in OptiFDTD by using the power transmission spectrum graph. Besides, the FDTD simulation also used in this simulation to show the results of resonance wavelength shift.

iii) Transmittance, T

The third parameter needs to consider is transmittance of PhC microcavity. It also determines the precision of the measurement of the sensing system in practical application [15]. Transmittance is calculated by dividing the output power (P_{out}) detected by the input power (P_{in}) of the source. Transmission spectra can be expressed as [15,16]:

$$T = P_{out}/P_{in} \tag{2.3}$$

The value of T will decrease when the coupling losses are considered between PhC microcavity and single mode fibers.

3.0 METHODOLOGY

In this work, we will using the ultra-compact and high sensitivity PCC as a technique to study the physical parametric of PhCC affecting the performance of sensor applications. Based on literature review, a micro RI gas sensor is designed in a 2D PhCC with triangular lattice. The radius of air holes is carefully to be designed in order to realize high sensitivity and appropriate measurement range. The microcavity can be formed by varying the radius of center air holes. In the other hand, the higher transmission efficiency can be realized by optimizing the parameters of the waveguides. The sensor also needs to have high transmission effiency and Q factor, which is could make the detection easy and feasible. The Q factor is defined as $\omega_0/\Delta\omega$, where $\Delta\omega$ is full width at half-maximum (FWHM) of the resonator's Lorentzian response, and ω_0 is TE resonance frequency. The FDTD simulation also used to show the results of the resonance wavelength shift.

3.1 Design Layout and Simulation in OptiFDTD

OptiFDTD is a software that has be used in designing PhCC and run all the simulations. The OptiFDTD software is based on the finite-difference time-domain (FDTD) method. The FDTD method is used for integrated and diffractive optic device simulations. The abilities of OptiFDTD is to model the propagation of light, scattering and diffraction, and reflection and polarization effects. Fig.2 below shows the flow chart for FDTD simulation in OptiFDTD software. This flow chart also explain in details the work flow in OptiFDTD.

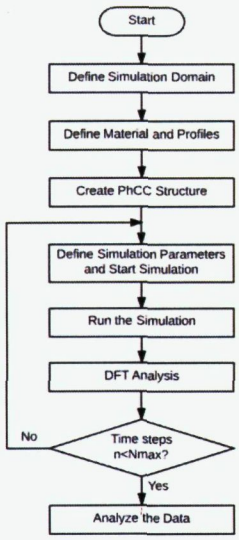

Fig.2: FDTD simulation flow chart in OptiFDTD

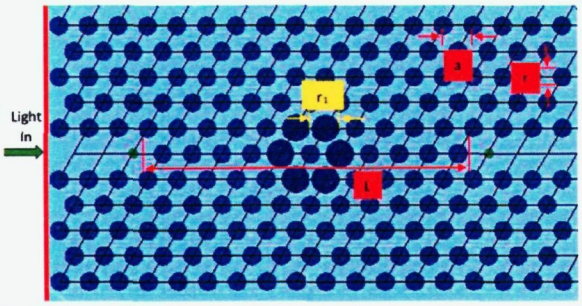

Fig.3: The specific structure of PhC microcavity.

Fig.3 showing the PhC microcavity slab structure designed for various sensing material such as gas, liquid and protein sensor. It is constructed using silicon slab with refractive index silicon, n_{si}=3.48. In this design the lattice constant is a=351nm, the radius of bulk air hole is r=0.3a=105.3nm and the thickness of PhCC slab h=0.6a=210.6nm. In this design, by increasing the radii of defected holes, r_1, PhC microcavity will be achieved and will be transformed to form a ring microcavity structure. Some air holes in the central of the row are symmetrically removed in order to enhance the coupling strength between the ridge waveguide and the length of waveguide is defined as L. This PhC microcavity is designed and analyzed by using OptiFDTD software [16]. All the calculations are using TE-polarization state and the time step is set to be 10000 with resolution 100. All the structures and simulation parameters, exclude for the parameters of defected holes are using the same setting which is number of defected holes, N=6, radii of defected holes, r_1=0.45a and length of waveguide, L=11a.

In this paper, the output transmission spectra of PhC microcavity for the different refractive index of defected holes has been calculated to show a better demonstration of RI sensing property. In the simulations, the vertical input plane is placed at the front of the observation point 1 and the observation point 2 is located at the output waveguide as shown Fig.3. Transmission spectra are calculated by dividing

the output power detected by the observation point 2 by the input power of the observation point 1 [17]. This simulation is done for 3 sensing material which is for gas, liquid, and protein.

3.2 Physical Parametric Studies of PhCC

In this project, there are three physical parametric studies of photonic crystal cavity that has been investigated in gas, liquid and protein sensing application. The purpose of these physical parametric studies is to analyze the performances of photonic crystal cavity for sensor application.

i) Increase the Refractive Index of Sensing Material, RI

The first physical parametric study is increased the refractive index of sensing material. The type of sensing material will be different according to its sensor application. Cryptophane E usually used to detect the concentration of methane gas. Therefore for gas sensor, we choose cryptophane E infiltrated to the defected holes of the PhCC. Sugar-water solution has been choose to infiltrate the defected holes of PhCC in order to perform the liquid sensor and the phosphate buffered saline (PBS) has been choose for protein sensor. The refractive index of the sensing material is determine its concentration.

ii) Increase the Radii of Defected Holes, r_1

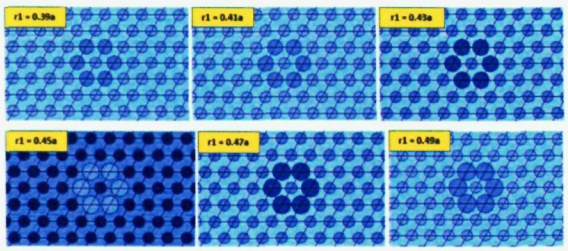

Fig.4: Specific layout radii of defected holes when r_1 = 0.39a, 0.41a, 0.43a, 0.45a, 0.47a and 0.49a.

Second physical parametric study is increased the radii or the radius of the defected holes. Fig.4 above shows the specific layout when we increased the radii of defected hole from $0.39a$ until $0.49a$. In this condition, the refractive index of the sensing materials will used the standard refractive index of its sensing material and for the number of defected holes we will used N=6 as the reference for this simulations.

iii) Increase the Number of Defected Holes, N

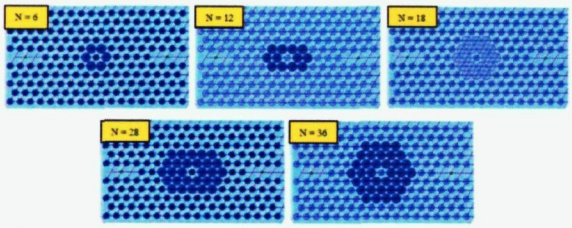

Fig.5: Specific layout the number of defected holes when N=6, 12, 18, 28, and 36.

The third physical parametric study is increase the number of defected holes. Fig.5 above shows the specific layout when we increased the number of defected holes from 6 until 36. In this condition, the refractive index material and the radii of the defected holes will used from the previous simulation.

3.3 Performance of PhCC

As stated in the objectives earlier, the purposed of this work are to study the changes of the physical parametric of PhCC structure will affecting the performances of the PhCC. In each physical parametric studies we will perform all these three performance in order to get the final structure of each sensor applications. There are three types of performances of PhCC that has been investigated in this work which are:

i) Refractive Index, RI Sensitivity

Refractive index sensitivity is the first performance that has been calculated. The data for time domain that has been collected from the simulation to calculate this performance. In order to analyze the RI sensitivity of the PhC microcavity structure, the resonant wavelength shift ($\Delta\lambda$) and the variation of refractive index (Δn) need to be observed. There are two ways to calculate this performance which is by using Equation (2.1) or using Microsoft Excel program to calculate slope for each curve of each refractive index. The slope of each curve for each refractive index represents the sensitivity of the specified PhC microcavity. In theoretically, the largest slope and maximum sensitivity will occur for larger radius of defected holes.

ii) Quality Factors, Q

The second performance is the quality factor. The Q factor can be calculated by using the Equation (2.2) which by dividing the resonant wavelength (λ) with the full width at half-maximum (FWHM) of the drop waveguide output ($\Delta\lambda$). The resonant wavelength and the bandwidth can be measured in OptiFDTD by using the power transmission spectrum graph and then the Q factor value can be calculated as shown in Fig.6.

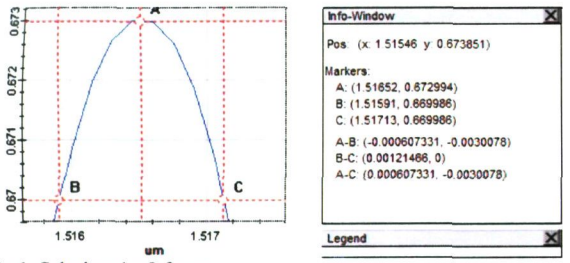

Fig.6: Calculate the Q factor

By referring Y plane coordinate for A, B, and C in Fig.6, we can then applying the Equation (2.2) to calculate the Q factor value. Besides, in this simulation to show the results of resonance wavelength shift we also can use the FDTD simulation.

iii) Transmittance, T

The third performance is the transmittance. Transmittance is calculated by using Equation (2.3) which is dividing the output power ($Pout$) detected with the input power (Pin) of the source. In theoretically, the value of T will be decrease when the coupling losses are considered between PhC microcavity and single mode fibers.

4.0 RESULTS AND DISCUSSION

4.1 Gas sensor

In gas sensor application, the cryptophane E is infiltrated at the central defected holes and the radii of defected holes will be altered to enhance the resonant property of PhC microcavity. We used refractive index of air to obtain the gas sensing, $n_{air} = 1$ to each bulk air holes. There are three physical parametric conditions has been investigated in order to see the performance of PhCC which are when we increased the refractive index, RI of sensing material, increased the radii of defected holes and lastly increased the number of defected holes.

i) Increase the refractive index (RI) of cryptophane E, S_n

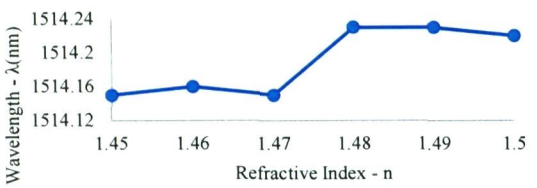

Fig.7(a): Resonant wavelength of PhC microcavity (r_1=0.45a, N=6) when the RI ranged from 1.45 to 1.50 with an increment of Δn=0.01.

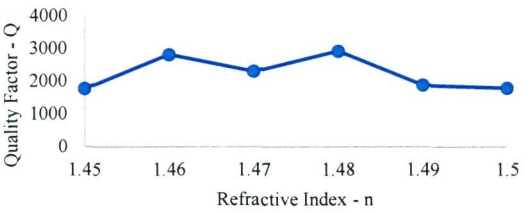

Fig.7(b): Q factor of PhC microcavity (r_1=0.45a, N=6) when the RI ranged from 1.45 to 1.50 with an increment of Δn=0.01.

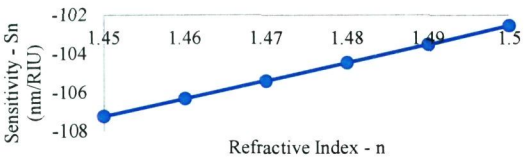

Fig.7(c): RI Sensitivity results when the RI of cryptophane E ranged from 1.45 to 1.50.

Fig.7(a),(b) and (c) shows the resonant wavelength, Q factor and RI sensitivity of PhC microcavity when RI is ranged from 1.45 to 1.50 with increment of $\Delta n = 0.01$. By increased the RI of the defected holes, the resonant curve shows shifted to the highest wavelength. This is shows that by varying the RI of defected holes will affecting the effective RI of membrane waveguide and photonic band structure because of the change of RI between Si substrate and air holes. For Fig.7(b), the Q factor values does not decreased greatly. As seen in Table 1 below, in this condition the RI sensitivity, S_n is about -102.54 nm/RIU, and the Q factor of the PhC microcavity is calculated around 2912. The RI sensitivity also represent as a slope of a curve. Therefore, from Fig.7(c) in order to get the RI sensitivity results we take the value of the slope for each curve of each RI of cryptophane E. In this results, it is shows the ability of cryptophane E infiltrated PhC microcavity as a gas sensor.

Table 1
Results of the performances when increased the RI of cryptophane E.

Performance	Results
RI Sensitivity, S_n	-102.54 nm/RIU
Quality factor, Q	2912

Future simulation is shows the property of gas sensor which is RI sensitivity (S_n), quality factor (Q), and normalized transmittance (T) by changed the radii of defected holes (r_1) and increased the number of defected holes (N). All the future simulations will used $n = 1.48$ which is RI of cryptophane E in non-methane environment.

ii) Increase the radii of defected holes, r_1

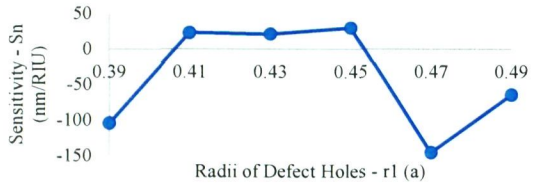

Fig.8(a): RI sensitivity of PhC microcavity (N=6) when radii of defected hole r_1 is ranged from 0.39a to 0.49a.

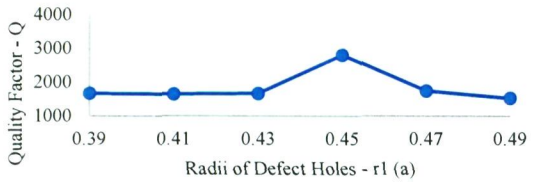

Fig.8(b): Q factor of PhC microcavity (N=6) when radii of defected hole r_1 is ranged from 0.39a to 0.49a.

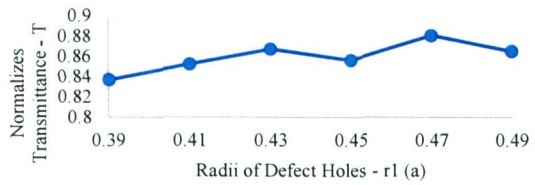

Fig.8(c): Normalized transmittance of PhC microcavity (N=6) when radii of defected hole r_1 is ranged from 0.39a to 0.49a.

Fig.8(a),(b) and (c) shows the simulation of S_n, Q, and T with changed of defected hole radius r_1. The r_1 is increased from $0.39a$ to $0.49a$ with an interval of $0.02a$ and all structure has been simulated to obtain the variation rules of their optical characteristics. From the simulation, it is shows all the three parameter is firstly increased then decreased with the increase of r_1. Table 2 shows the result of this performances which radii of defect holes are obtained the optimal value.

Table 2
Result of the performances which of the radii of defect holes are obtained the optimal value.

Performances	Radii of defect holes, r_1
RI Sensitivity, S_n	0.45a
Quality factor, Q	0.45a
Transmittance, T	0.47a

As seen in Table 2, S_n and Q obtain largest value when $r_1 = 0.45a$ with $S_n = 29.9$ nm/RIU and $Q = 2804$. While T obtained the largest value when $r_1 = 0.47a$ with $T = 0.8806$. Therefore, in the following simulations, the radius of defected holes r_1 will be set to $r_1 = 0.45a$ as the optimal cavity structure. Next, the relationship between the properties of PhC microcavity and the number of defected holes N is investigated when the radius of defected holes $r_1 = 0.45a$.

iii) Increase the number of defected holes, N

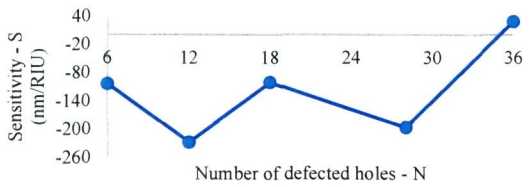

Fig.9(a): RI sensitivity of PhC microcavity ($r_1 = 0.45a$) when N=6, 12, 18, 28, and 36.

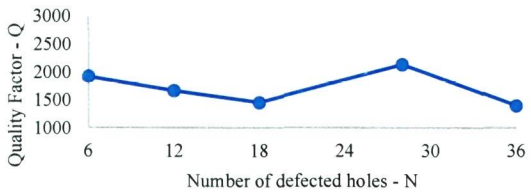

Fig.9(b): Q factor of PhC microcavity ($r_1 = 0.45a$) when N=6, 12, 18, 28, and 36.

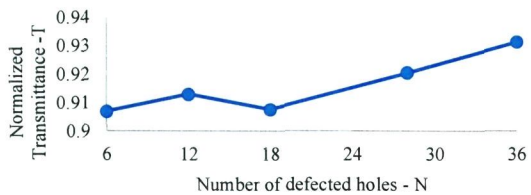

Fig.9(c): Normalized transmittance of PhC microcavity ($r_1 = 0.45a$) when N=6, 12, 18, 28, and 36.

The graphs in Fig.9(a),(b) and (c) shows the calculated S_n, Q, and T when the value of defected holes N=6, 12, 18, 28, and 36. As shown in Fig.9(a) and (c), the changed of N will changed the RI sensitivity and T of resonant mode and $N = 36$ is the optimal design with $S_n = 28.79$ nm/RIU and $T = 0.9312$. The RI sensitivity shows that S_n is larger for the biggest number of defected holes N. By refer to Fig.9 (a) the S_n is increases rapidly at $N = 36$ compared to other defected holes. Therefore in this PhC microcavity design, $N = 36$ is acts as marking point.

Table 3
Result of the performances which of the number of defected holes are obtained optimal value.

Performances	Number of defected holes, N
RI Sensitivity, S_n	36
Quality factor, Q	28
Transmittance, T	36

iv) Final PhCC structure for gas sensor

In this final PhC microcavity structure, we takes all the optimal value of the previous performance results of each conditions. Therefore as a conclusion, the final PhC microcavity structure for gas sensor that has been employed is when cavity with $r_1 = 0.45a$ and $N = 36$. By using this parameters, the designed PhC microcavity has RI sensitivity of 48.2 nm/RIU, quality factor of 2551 and transmission of 0.3330.

Table 4
Final results of the performances for final PhC structure of gas sensor.

Performances	Final result
RI Sensitivity, S_n	48.2 nm/RIU
Quality factor, Q	2551
Transmittance, T	0.3330

4.2 Liquid sensor

In liquid sensing application, we used sugar-water solution as a receptor infiltrated at the center of defected holes. The concentration of sugar-water solution is determine by the refractive index.

i) Increase the RI of sugar-water solution, S_n

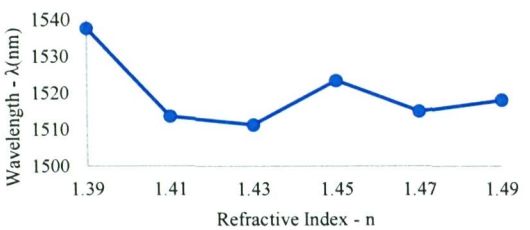

Fig.10(a): Resonant wavelength of PhC microcavity (r_1=0.45a, N=6) when the RI ranged from 1.39 to 1.49.

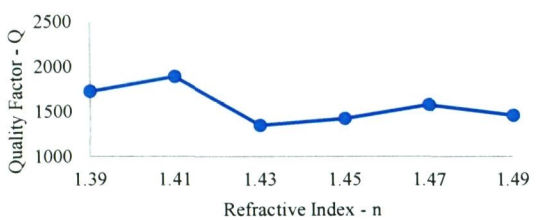

Fig.10(b): Q factor of PhC microcavity (r_1=0.45a, N=6) when the RI ranged from 1.39 to 1.49.

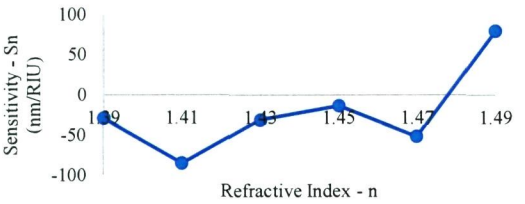

Fig.10(c): RI Sensitivity of PhC microcavity (r_1=0.45a, N=6) when the RI ranged from 1.39 to 1.49.

Fig.10(a),(b) and (c) shows the resonant wavelength, Q factor and RI sensitivity of PhC microcavity when RI is ranged from 1.39 to 1.49 with increment of $\Delta n = 0.02$. For Fig.10(b), the Q factor values decreased greatly at $n = 1.41$ to $n = 1.43$ then it increase slowly. In this condition, the RI sensitivity, S_n is about 79.6 nm/RIU, and the Q factor of the PhC microcavity is calculated around 1892. This shows the ability of sugar-water solution infiltrated PhC microcavity as a liquid sensor.

Table 5
Results of the performances when increased the RI of sugar-water solution.

Performance	Results
RI Sensitivity, S_n	79.6 nm/RIU
Quality factor, Q	1892

Future simulation is shows the property of liquid sensor which is RI sensitivity (S_n), quality factor (Q), and normalized transmittance (T) by change the radii of defected holes (r_1) and increased the number of defected holes (N). All the future simulations will used $n = 1.47$ which is RI of sugar-water solution.

ii) Increase the radii of defected holes, r_1

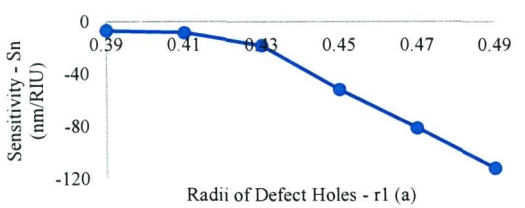

Fig.11(a): RI sensitivity of PhC microcavity (N=6) when radii of defected holes r_1.

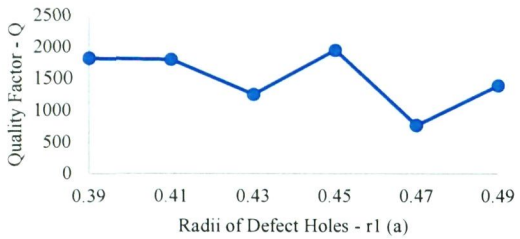

Fig.11(b): Q factor of PhC microcavity (N=6) when radii of defected holes r_1.

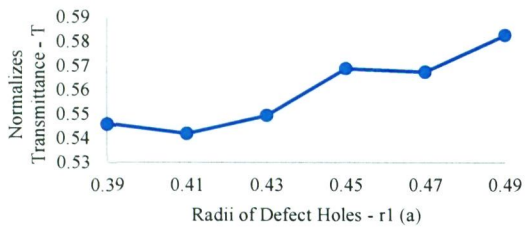

Fig.11(c): Normalized transmittance of PhC microcavity (N=6) when radii of defected holes r_1.

Fig.11(a),(b) and (c) shows the simulation of S_n, Q, and T with changed of defected hole radius r_1. The radius of defected holes r_1 is increased from $0.39a$ to $0.49a$ with an interval of $0.02a$ and all structures has been simulated to obtain the variation rules of their optical characteristics.

Table 6
Result of the performances which of the radii of defect holes are obtained the optimal value.

Performances	Radii of defect holes, r_1
RI Sensitivity, S_n	0.39a
Quality factor, Q	0.45a
Transmittance, T	0.45a

From the simulation, Q and T obtain the higher increment value for the radius of defected holes is when $r_1 = 0.45a$ with $Q = 1942$ and $T = 0.5825$. While S_n obtain the largest value when $r_1 = 0.39a$ with $S_n = 1816$. Therefore, in the following simulations, the radius of defected holes r_1 will be set to $r_1 = 0.45a$ as the optimal cavity structure.

iii) Increase the number of defected holes, N

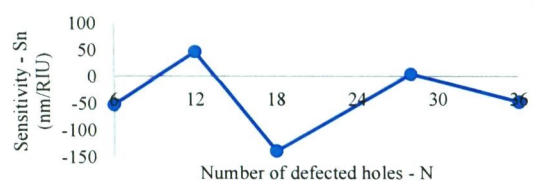

Fig.12(a): RI sensitivity of PhC microcavity ($r_1 = 0.45a$) when N=6, 12, 18, 28, and 36.

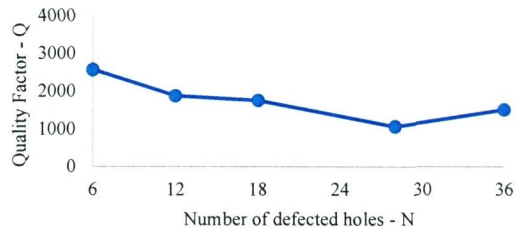

Fig.12(b): Q factor of PhC microcavity ($r_1 = 0.45a$) when N=6, 12, 18, 28, and 36.

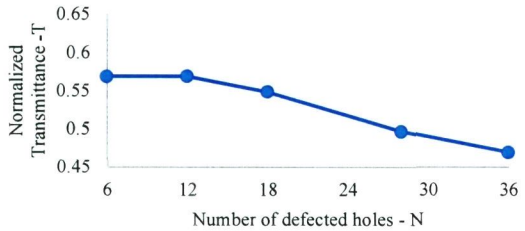

Fig.12(c): Normalized transmittance of PhC microcavity ($r_1 = 0.45a$) when N=6, 12, 18, 28, and 36.

The relationship between the properties of PhC microcavity and the number of defected holes N is investigated when the radius of defected holes $r_1 = 0.45a$. Graphs in Fig.12(a),(b) and (c) shows the calculated S_n, Q, and T when the value of defected holes N=6, 12, 18, 28, and 36. As shown in Fig.12(a) and (c), the changed of N will changed the S_n and T of resonant mode and $N = 12$ is the optimal design with $S_n = 46.3$ nm/RIU and $T = 0.5690$. The RI sensitivity shows that $S_n$is larger for the small number of defected holes N. By refers to Fig.12(a) the S_n value is high at $N = 12$ compared to other defected holes. Therefore in this PhC microcavity design, $N = 12$ is acts as marking point.

Table 7
Result of the performances which of the number of defected holes are obtained optimal value.

Performances	Number of defected holes, N
RI Sensitivity, S_n	12
Quality factor, Q	6
Transmittance, T	12

iv) Final PhC structure for liquid sensor

In this final PhC microcavity structure, we takes all the optimal value of the previous performance results of each conditions. Therefore as a conclusion, the final PhC microcavity structure for liquid sensor that has been employed is when cavity with $r_1 = 0.45a$ and $N = 12$. By using this parameters, the designed PhC microcavity has RI sensitivity of 46.3 nm/RIU, quality factor of 1874 and transmission of 0.5690.

Table 8
Final results of the performances for final PhC structure of liquid sensor.

Performances	Final result
RI Sensitivity, S_n	46.3 nm/RIU
Quality factor, Q	1874
Transmittance, T	0.5690

4.3 Protein sensor

In protein sensing application, we used phosphate buffered saline (PBS) infiltrated the defected holes of PhC microcavity to observe protein. The concentration of PBS is determine by the refractive index.

i) Increase the RI of phosphate buffered saline (PBS), S_n

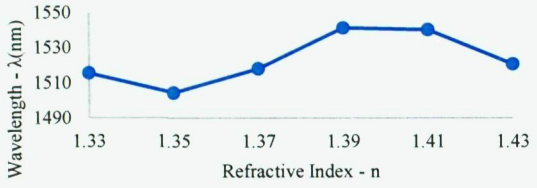

Fig.13(a): Resonant wavelength of PhC microcavity (r_1=0.45a, N=6) when the RI ranged from 1.33 to 1.43.

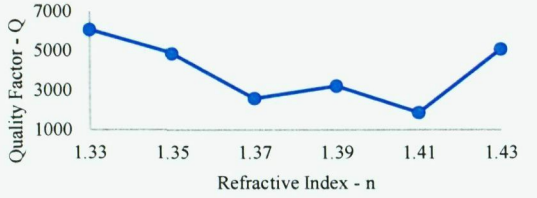

Fig.13(b): Q factor of PhC microcavity (r_1=0.45a, N=6) when the RI ranged from 1.33 to 1.43.

Fig.13(c): RI sensitivity of PhC microcavity (r_1=0.45a, N=6) when the RI ranged from 1.33 to 1.43.

Fig.13(a),(b) and (c) shows the resonant wavelength, Q factor and RI sensitivity of PhC microcavity when RI is ranged from 1.33 to 1.43 with increment of $\Delta n = 0.02$. For Fig.13(b), the Q factor values decreased greatly from $n = 1.33$ to $n = 1.37$ then it increase slowly. In this case, the RI sensitivity, S_n is about 189.5 nm/RIU, and the Q factor of the PhC microcavity is calculated around 6062. This shows the ability of phosphate buffered saline (PBS) solution infiltrated PhC microcavity as a protein sensor.

Table 9
Results of the performances when increased the RI of PBS solution.

Performance	Results
RI Sensitivity, S_n	189.5 nm/RIU
Quality factor, Q	6062

Future simulation is shows the property of protein sensor which is RI sensitivity (S_n), quality factor (Q), and normalized transmittance (T) by change the radii of defected holes (r_1) and increased the number of defected holes (N). All the future simulations will used $n = 1.35$ which is RI of PBS solution.

ii) Increase the radii of defected holes, r_1

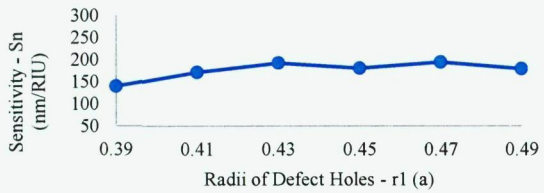

Fig.14(a): RI sensitivity of PhC microcavity (N=6) when radii of defected holes r_1.

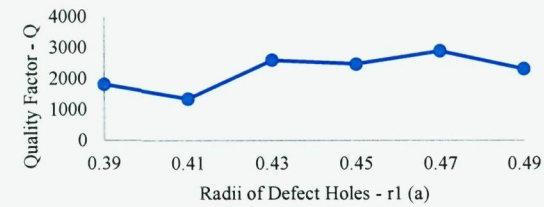

Fig.14(b): Q factor of PhC microcavity (N=6) when radii of defected holes r_1.

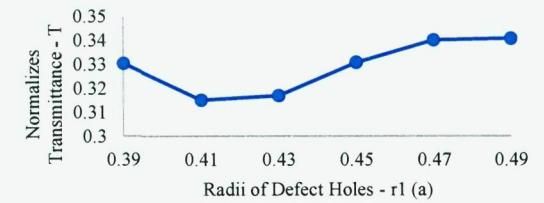

Fig.14(c): Normalized transmittance of PhC microcavity (N=6) when radii of defected holes r_1.

Fig.14(a),(b) and (c) shows the simulation of S_n, Q, and T with changed of defected hole radii r_1. The radius of defected holes r_1 is increased from $0.39a$ to $0.49a$ with an interval of $0.02a$ and all structures has been simulated to obtain the variation rules of their optical characteristics.

Table 10
Result of the performances which of the radii of defect holes are obtained the optimal value.

Performances	Radii of defect holes, r_1
RI Sensitivity, S_n	0.47a
Quality factor, Q	0.43a
Transmittance, T	0.45a

From the simulation, T obtain the higher increment value for the radius of defected holes is when r_1= $0.45a$ while Q obtain the largest value when r_1=$0.43a$ while $S_n = 0.47a$. Due to the results shows the different values of the performance therefore we choose the highest increment value and in the following simulations, the radius of defected holes r_1 will be set to r_1= $0.45a$ as the optimal cavity structure.

iii) Increase the number of defected holes, N

Fig.15(a): RI sensitivity, Q factor and normalized transmittance of PhC microcavity (r_1= 0.45a) when N=6, 12, 18, 28, and 36.

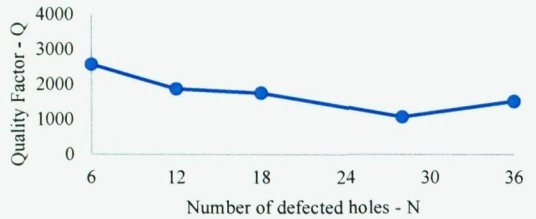

Fig.15(b): Q factor of PhC microcavity (r_1= 0.45a) when N=6, 12, 18, 28, and 36.

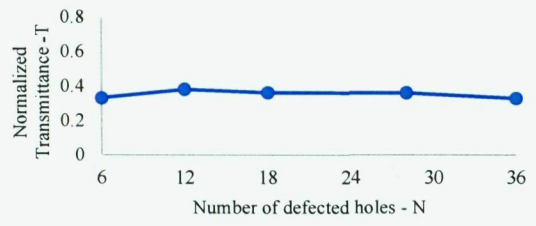

Fig.15(c): Normalized transmittance of PhC microcavity (r_1= 0.45a) when N=6, 12, 18, 28, and 36.

Then the relationship between the properties of PhC microcavity and the number of defected holes N is investigated when the radius of defected holes $r_1 = 0.45a$. Graphs in Fig.15(a),(b) and (c) shows the calculated S_n, Q, and T when the value of defected holes N=6, 12, 18, 28, and 36. As shown in Fig.15(a) and (c), the changed of N will changed the S_n and T of resonant mode and $N = 12$ is the optimal design with $S_n = 114.4$ nm/RIU and $T = 0.3814$. The RI sensitivity shows that $S_n$is larger for the small number of defected holes N. By refer to Fig.15(a), the S_n is increased at $N = 12$ compared to other defected holes. Therefore in this PhC microcavity design, $N = 12$ is acts as a setting point.

Table 11
Result of the performances which of the number of defected holes are obtained optimal value.

Performances	Number of defected holes, N
RI Sensitivity, S_n	12
Quality factor, Q	6
Transmittance, T	12

iv) Final PhC structure for protein sensor

In this final PhC microcavity structure, we takes all the optimal value of the previous performance results of each conditions. Therefore as a conclusion, the final PhC microcavity structure for protein sensor that has been employed is when cavity with r_1= $0.45a$ and $N = 12$. By using this parameters, the designed PhC microcavity has RI sensitivity of 114.4 nm/RIU, quality factor of 1659 and transmission of 0.3814.

Table 12
Final results of the performances for final PhC structure of protein sensor.

Performances	Final result
RI Sensitivity, S_n	114.4 nm/RIU
Quality factor, Q	1659
Transmittance, T	0.3814

4.4 Comparison result for each sensing applications

Table 13
Comparison results from our optimized PhC microcavity for various sensing material.

Sensing material	RI sensitivity (nm/RIU)	Quality factor	Normalized transmission
Gas	48.2	2551	0.3330
Liquid	46.3	1874	0.5690
Protein	114.4	1659	0.3814

Based on the theoretical, this structure of PhC microcavity is designed for gas sensing application using cryptophane E to detect the methane gas [18]. Zhang et al. state that heterostructure cavity has the highest $Q$and highest RI sensitivity among all of these PhC cavity structure [18,19,20,21,22,23]. This structure has been choose to

investigate other sensing material such as other gases, liquid and protein. Table 13 above shows the comparison of the results from various sensing material of PhC microcavity. From the table as can seen, this structure can be used in other sensing application. Q factor of gas sensor showing the highest value compare to other sensor. It prove that this structure is designed for gas sensing application [8]. From Table 13 it shows the comparison results from all simulations for different sensing material of PhC microcavity. As can seen, gas sensor shows the highest value for quality factor which is 2551 compare to other sensor. In the other hand, liquid sensor shows the highest normalized transmission value which is 0.5690 and protein sensor shows highest in RI sensitivity which is 114.4 nm/RIU.

Table 14
Comparison of resonant properties among the published PhC microcavities and our optimized PhC microcavity.

Structure	RI sensitivity (nm/RIU)	Quality factor	Sensing material	Publish year	Ref
L11 Ring Microcavity	363.8	1.3×10^4	Gas	2015	[18]
Heterostructure cavity	80	3.8×10^5	Gas	2008	[19]
Slotted Heterostructure cavity	510	2.6×10^4	Gas	2010	[20]
Modified L7 cavity	460	2.6×10^3	Liquid	2012	[21]
L3 cavity	98	6.5×10^3	Liquid	2010	[22]
H1 cavity	165.45	4×10^3	Liquid	2013	[23]
Our optimized cavity	48.2	2.6×10^3	Gas	-	-
	46.3	1.9×10^3	Liquid	-	-
	114.4	1.7×10^3	Protein	-	-

In this paper, we observe this resonator possesses a larger Q-factor which is at 2551 and a full width at half maxima less than a nanometer. This is due to the theoretical state that the higher Q-factor make it easier to detect very small shifts in the resonances [20]. In Table 14, we list the S_n and Q of some PhC microcavities that already stated in introduction, where our optimized PhC microcavity is also include in the comparison. As can seen, from the table it shows heterostructure cavity has the highest Q and highest RI sensitivity compare to other PhC cavity structure. Even though our optimize cavity does not shows the highest $Q$and highest RI sensitivity, but we proved that this sensing structure beside good as a gas sensing application it also good for protein sensor as well.

5.0 CONCLUSION

In this work, a few number of photonic crystal cavity structure have been designed and analysed and identified the physical parametric studies of the performances of this photonic crystal cavity. The main objective of this work was to design twp dimensional heterostructure ring microcavity of photonic crystal cavity and to optimize the design by introducing a defected holes of the photonic crystal cavity structure. Optimization has been justified by the calculation of refractive index sensitivity, quality factor and transmission. This work has been compared with the previously published work from other researchers on photonic crystal cavity especially for heterostructure structures of photonic crystal cavity. The design and analysis for all performance of photonic crystal cavity has been performed by using OptiFDTD software. In this work, we are studied about the application of analyte receptor that was infiltered in PhC microcavity for different sensing material. The RI sensitivity, quality factor and transmittance of the proposed cavity can be determine by using finite difference time domain (FDTD) method. Beside as a gas sensor of PhC microcavity application, this structure also can be used as a protein sensor. From the results it is shows for protein sensing, the RI sensitivity of 114.4 nm/RIU has been observed.

5.1 Recommendation for Future Project

Suggestion for future project is to design in structure by using RSOFT software and fabricate this design to compare the theoretical result and practical results. In this work, the material used is silicon (Si) as the background methods. Recently, more advanced material system such as photonic crystal made of air spheres in titania (TiO2) [24], liquid-crystal photonic band gap [25], and many others can be added in PhC analysis. Besides, in future work is to include these modern material systems in the design and analysis.

REFERENCES

[1] Afroz, R., Hassan, M. N., & Ibrahim, N. A. (2003). Review of air pollution and health impacts in Malaysia. Environmental Sciences, 71-77.

[2] Golo von Basum, D. H. (2004). Parts per trillion sensitivity for ethane in air with an optical parametric oscillator cavity leak-out spectrometer. Optics Letters, Vol. 29, Issue 8, pp. 797-799.

[3] Pergande, D., Geppert, T., von Rhein, A., Schweizer, S., Ralf, B., Wehrspohn, R., Lambrecht, A. (2011). Miniature infrared gas sensor using photonic crystals. J. Appl. Phys, 109.

[4] Y.A. BakhirkinA.A. KosterevR.F. CurlF.K. Tittel, D. Y. (2006). Sub-ppbv nitric oxide concentration measurements using CW thermoelectrically cooled quantum cascade laser-based integrated cavity output spectroscopy. Applied Physics B, Volume 82, Issue 1, pp 149–154.

[5] Zahniser, D. N. (2002). Sub-part-per-billion detection of nitric oxide in air using a thermoelectrically cooled mid-infrared quantum cascade laser spectrometer. Applied Physics B, Volume 75, Issue 2, pp 343–350.

[6] Joannopoulos JD, J. S. (2008). *Photonic crystals: Molding the Flow of Light. 2nd edn.* Princeton University Press: Princeton.

[7] E., Y. (1987). Inhibited spontaneous emission in solid-state physics and electronics. *Phys Rev Lett.*, 58(20):2059-2062.
[8] S., J. (1987). Strong localization of photons in certain disordered dielectric superlattices. *Phys Rev Lett*, 58(23):2486-2489.
[9] Frazão O, S. J. (2008). Laser & Photon. *Rev*, 2:449–59.
[10] Pinto AMR, L. (2012). Sensors. 1–21.
[11] A. Casas-Bedoya, S. Shahnia, D. Di Battista, et al., Chip scale humidity sensing based on a microfluidic infiltrated photonic crystal, Appl. Phys. Lett. 103 (18) (2013) 181109 (1–4).
[12] S. Zheng, Y. Zhu, S. Krishnaswamy, Fiber humidity sensors with high sensitivity and selectivity based on interior nanofilm-coated photonic crystal fiber long-period gratings, Sens. Actuators, B: Chem. 176 (2013) 264–274.
[13] D. Wang, Z. Yu, Y. Liu, et al., Ultrasmall modal volume and high Q factor optimization of a photonic crystal slab cavity, J. Opt. 15 (12) (2013) 125102 (1–7).
[14] Kang, C., & Weiss, S. M. (2008). Photonic crystal with multiple-hole defect for sensor applications. Optics express, 16(22), 18188-18193.
[15] Olyaee, S., Mohsenirad, H., & Mohebzadeh-Bahabady, A. (2016). Photonic Crystal Chemical/Biochemical Sensors.
[16] http://www.dileepnanotech.com/electronics/electronic 2.html
[17] Kumar, P., Pathak, S. K., Meher, A. K., & Mohapatra,S. (2015, February). A unique design of PCF with zero dispersion and high birefringence. In Electronics and Communication Systems (ICECS), 2015 2nd International Conference on (pp. 123-125).
[18] Y. Zhang, Y. Zhao, Q. Wang, Measurement of methane concentration with cryptophane E infiltrated photonic crystal microcavity, Sens. Actuators, B: Chem. 209 (2015) 431–437.
[19] T. Sunner, T. Stichel, S.-H. Kwon, et al., Photonic crystal cavity based gas sensor, Appl. Phys. Lett. 92 (26) (2008) 261112 (1–3).
[20] J. Jagerska, H. Zhang, Z. Diao, et al., Refractive index sensing with an air-slotphotonic crystal nanocavity, Opt. Lett. 35 (15) (2010) 2523–2525.
[21] Y. Liu, H.W.M. Salemink, Photonic crystal-based all-optical on-chip sensor, Opt.Express 20 (18) (2012) 19912–19920.
[22] C. Kang, C.T. Phare, Y.A. Vlasov, et al., Photonic crystal slab sensor with enhanced surface area, Opt. Express 18 (26) (2010) 27930–27937.
[23] S. Olyaee, S. Najafgholinezhad, Computational study of a label-free biosensor based on a photonic crystal nanocavity resonator, Appl. Opt. 52 (29) (2013)7206–7213.
[24] Judith E. G. J. Wijnhoven, Willem L. Vos, "Preparation of Photonic Crystals Made of Air Spheres in Titania", Science 7 August 1998: Vol. 281 no. 5378 pp. 802-804, Van der Waals-Zeeman Institute, University van Amsterdam, Valckenierstraat 65, NL-1018 XE Amsterdam, Netherlands.
[25] Kurt Busch and Sajeev John, "Liquid-Crystal Photonic-Band-Gap Materials: The Tunable Electromagnetic Vacuum", Published 2 August 1999, Volume 83, Number 5, Department of Physics, University of Toronto, 60 St. George Street, Toronto, Ontario, Canada M5S 1A7.